Egyptian Journal of Chemistry

http://ejchem.journals.ekb.eg/

Evaluation of the Cytotoxicity of Mesoporous Silica Nanoparticles Loaded With Gallic Acid on Laryngeal Cancer (HEP-2) Cell Lines

Heba M. Fahmy*; Manar M. Hamed; Ahmed S. Monem
Biophysics Department, Faculty of Science, Cairo University, Giza, Egypt

Abstract

Gallic acid (GA), is a polyphenolic compound exceptionally well absorbed compared with other polyphenols, and it has many biological and pharmacological activities, it is renowned for its antioxidant, anticancer, anti-inflammatory, and antibacterial properties. Mesoporous Silica Nanoparticles (MSNs) of varied sizes, produced with variable amounts of NH3OH, are used in this study to deliver GA intracellularly and explore its cytotoxicity to specifically target laryngeal cancer cells (HEP-2), these MSNs were loaded with GA. The GA-loaded MSNs were characterized using Dynamic Light Scattering (DLS) analysis and Scanning Electron Microscopy (SEM). The encapsulation efficiency of GA within the MSNs was determined using High-Performance Liquid Chromatography (HPLC). The cytotoxicity of both the MSNs and GA-loaded MSNs was evaluated at concentrations ranging from 4.5 to 10000 µg/ml using the MTT assay over 72 hours on HEP-2 cells. Our findings revealed that   MSN sizes increased as a result of NH₃OH-increased MSNs. The viability of HEP-2 cells was seen to decrease at high concentrations of MSNs and MSN-GA and increase at low concentrations., particularly the smaller MSN1, demonstrated high encapsulation efficiency for GA and lower toxicity than MSN2 and MSN3. This underscores the potential of small MSNs to enhance drug delivery without inducing cellular damage. Notably, the structural integrity of GA was maintained upon encapsulation within the MSN pores. GA-loaded MSN2 and MSN3 demonstrated comparable anticancer efficacy to free GA, and following intracellular uptake, the GA-loaded MSNs could release GA into the cells. In conclusion, due to their small size and high encapsulation efficiency, MSNs emerge as ideal nanocarriers for GA delivery. The cellular uptake of GA-loaded MSNs was studied by MTT test and results showed their high biocompatibility This presents a promising therapeutic strategy for the treatment of HEP-2 human laryngeal carcinoma cells, leveraging the natural antioxidant properties of GA..

Keywords: Gallic acid (GA); laryngeal cancer (HEP-2); Mesoporous Silica Nanoparticles (MSN); cytotoxicity

---

1. Introduction

One kind of cancer that attacks the tissues of the larynx is called laryngeal cancer, or laryngeal carcinoma It is the second most frequent cancer in the upper aerodigestive tract. Laryngeal carcinoma is the term for the situation when carcinoma cells form in the tissues of the larynx [1]**.** Every cancer starts with a mutation in a cell's DNA. Our cells get their fundamental set of instructions from DNA, including when to divide and proliferate. The instructions that regulate cell growth can be changed by a mutation in DNA, which causes cells to proliferate instead of stopping when they should. This leads to the cells proliferating uncontrollably, resulting in the formation of tissue known as cancer [2]. Antioxidant gallic acid is categorized as a secondary polyhydroxy phenolic [3]**.** Plants contain GA in either its free-state or ester form [4] It is available in a variety of fruits and vegetables [5] [6]. GA is exceptionally well absorbed compared with other polyphenols, and it has many biological and pharmacological activities, such as a potent antioxidant effect, antimicrobial, gastroprotective, anti-inflammatory, anti-HIV, and anticancer [8,14,15]. GA scavenges free radicals, which lowers oxidative stress, including hydroxyl (HO) and superoxide (O2.−), two examples of reactive oxygen species (ROS). also, by scavenging oxidizing molecules that are not radical, including hydrogen peroxide (H2O2) [9] Free radical buildup and excessive H2O2 can cause DNA damage to cells, which can result in mutations that start and encourage carcinogenesis GA possesses redox characteristics and metal chelation, which cause cancer cells to undergo apoptosis, among its other antioxidative effects [10,17] It has been observed that GA can protect DNA and cells from oxidative damage at low doses. However, GA itself has the potential to harm DNA and cells in larger quantities [11,18]. GA's poor bioavailability and permeability, restricted absorption, and quick metabolism are the primary obstacles to its usage as a prodrug. These are caused by the hydrophilic qualities of GA, which hinder its passive diffusion over the gut tract. [12]. Although numerous studies have demonstrated that GA is both safe and effective, its pharmacokinetic properties of it is the poor absorption, low bioavailability, and rapid metabolism, the drug received is low in concentrations, and therefore its removal is too fast [13]**[20]** [16]. Therefore, it is clear that there is a need to create transport methods that ensure both the protection and controlled release of GA. Encapsulating GA in nanoparticles makes sense to effectively increase its bioavailability and boost therapeutic output in cancer tissue by enhancing its absorption via transcellular or paracellular processes [13]. Over the past few decades, the use of drug delivery systems made possible by nanotechnology has drawn more and more attention. It is being used in more and

---

_____

more tumour-targeted applications [19]. It has significant benefits for cancer treatment, such as drug resistance, targeting cancer cells with high accuracy, and minimizing adverse effects **[21].** MSNs are among the extensively studied applications of inorganic nanoparticles in medicine **[22,23,24].** Its many positive traits help improve the drug's properties, such as its ability to resist external hydrolysis, pH, thermal, and mechanical stress due to the particle morphology and its inorganic robust framework [**25,26**].

The MSNs have a particle size distribution of (50–300) nm., whose structure allows for endocytosis-mediated uptake by live cells **[27].** Uniform porous structure, big pore size, and surface area allow for high drug loading, improved dissolving rate, and water-soluble loading; so, in the treatment of cancer, it was utilized to transport drugs that had low solubility in water **[27,28,29].** MSNs are negatively charged, which enhances their permeability and retention in the tumor tissue **[30].** The Food and Drug Administration in the United States has deemed MSN safe for consumption, so it is biocompatible and biodegradable, has good encapsulation, and is easy to form **[28].** Its production is easy and inexpensive **[27].** These properties have made mesoporous widely used in many biomedical applications and other fields, such as gene therapy, photodynamic therapy **[6]**, tumor therapy **[31]**, bioimaging **[32],** and stem cells **[33].**

There are many different ways to treat cancer: radiotherapy, surgery, chemotherapy, and targeted cancer drugs. When the drug is taken orally or injected, it will enter the circulatory system, causing side effects that cannot be controlled **[6].** Due to the high ability of the MSN to load a large amount of the drug, especially the hydrophobicity, this property can prevent poisoning of healthy tissues. Their appealing features make MSNs exciting options for improving cancer therapy **[34].** Studies have shown that the silanol groups on the surface of MSNs, which could connect accidentally to specific proteins on the cell membrane and cause cell death, are primarily responsible for the cytotoxicity of MSNs **[35].** Zeta potential, surface modification, and particle size significantly affected MSN cytotoxicity **[6].**

MSN Synthetic Manufacturing done by Alkoxysilanes are hydrolyzed, and the hydrolysis products are then condensed. Various techniques are used for this process, including the Stöber method (sol-gel method), hydrothermal synthesis methods, and micro-emulsion **[36,37].** MSNs provide an essential tool for the managed release of different medicines. The particle size and distribution are dependent on the processing conditions of the MSNs; therefore, in this work, We Study How Ammonia Volume Affects MSN Size were synthesized by the Stöber method and then loaded gallic acid into the pores of the three different sizes of mesoporous materials, MSN1 and MSN2, and MSN3, and evaluate their release and cytotoxicity into human larynx carcinoma cells (HEP-2) with MTT assay.

2. Materials and Methods
2.1. Materials

Ammonia hydroxide 28% ($NH_4 OH$), N- cetyl tri methyl ammonium bromide (CTAB), tetra ethoxy ortho silicate (TEOS), Gallic acid, and Dimethyl sulphoxide (DMSO) acquired from Sigma Aldrich, Germany. 96% Ethoxy Ethanol ($C_4H_{10}O_2$) acquired from Diachem Chemicals, USA. (Di methyl thiazole-2-yl)-2, 5-diphenyltetrazolium bromide) (MTT), Ethanol (C_2H_5OH), (PSB) Phosphate buffer pH 7.4, cellulose ester dialysis bag was obtained from Sigma CO. Ltd. (USA).

2.2. Methods
2.2.1 Preparation of MSNs

Three sizes of MSNs were prepared: MSN1, MSN2, and MSN3. Briefly, In 70 ml of distilled water, 0.5 g of CTAB was dissolved, placed on a magnetic stirrer, and heated to 50 degrees Celsius to dissolve CTAB; after that, we just let the solution cool down. For MSN1, we mixed 0.25 ml of 28% ammonium hydroxide with 30 ml of ethoxy ethanol and stirred the mixture for 30 minutes. Then, 2.5ml TEOS was added to each sample. Samples were left for 24 hours on a magnetic stirrer. After 24h, samples were preserved in the refrigerator until the next day to permit the swelling of the MSN. Using deionized water and ethanol, samples were washed three times before being dried at 80 degrees Celsius for 24 hours at room temperature. Calcination was used to remove the surfactant. The calcination process for MSNs started at 25°C and then heated to 550 °C at a rate of 1 °C/min was achieved for 4 hours. Other MSNs: MSN2 and MSN3 were prepared following the same process outlined above but by adding (0.5 ml) Ammonia hydroxide 28% to prepare MSN2 and (1 ml) Ammonia hydroxide 28% to prepare MSN3.

2.2.2. Loading of Gallic acid on MSNs

(10 mg) of MSN1 (40 mg/ ml) of GA- ethanol was added at room temperature in darkness and stirred for 48 hours at 100 rpm. MSN-GA1 was washed thrice with ethanol by centrifugation at room temperature at 8000 rpm. 1µl of the ethanol was used to dilute the filtrate to 10 ml, and the amount of loaded GA was determined by (UV/V) spectroscopy at 272 nm. The same method described above was used for MSN2 and MSN3.

2.3. Characterization of the prepared formulations
2.3.1. Encapsulation efficiency calculation (EE %)

The efficiency of encapsulation for MSN1, MSN2, and MSN3 was figured out by centrifuging. The samples were spun at 8,000 RPM for 30 minutes (VS-18000M, Korea, 220 V/50 HZ) to remove the samples from the supernatant. The clear residue was then gathered and stirred to get a mixture that was all the same. After centrifugation, the pellets were mixed with 10 ml of saline buffer (pH 7) and sonicated for 10 minutes. HPLC (Young Lin Instrument, Korea) measured the free drug concentration in the solution for the MSN1, MSN2, and MSN3 samples. The following equation was used to figure out how well they were encapsulated:

_____

_____

$$\text{Encapsulation efficiency \% } = (\frac{\text{initial concentration} - \text{supernatant concentration}}{\text{initial concentration}}) \times 100 \text{ \%}$$

2.3.2. Particle size and zeta potential

Malvern Instruments' Zetasizer Nano ZS90 was used to quantify the zeta potential and particle size of the MSN1, MSN2, and MSN3 samples using dynamic light scattering (DLS) analysis. Before analysis, each sample was diluted with the necessary volume of deionized water. Following three measurements of each sample, the means and standard errors of the means were computed.

2.3.3. Scanning electron microscopy (SEM)

MSNs and MSNs-GA were examined using an SEM (Philips xl-30) to determine their structure and particle shape.

2.3.4. In-vitro drug release

The dialysis bag method was employed to assess the GA release from MSNs by adding 10 mg of MSNs-GA inside the dialysis bag containing 1ml of ethanol and 4ml of PBS (pH 7.4) and then suspending the dialysis bag in 15-ml PBS in tubes and at 37 °C stirred it for 84h and then determined the released of GA from MSNs by the spectrometer at 274 nm every thirty minutes.

2.3.5 The MTT assay

The MTT experiment is a colorimetric method that measures cell viability, a quantitative and reliable technique. Evaluating MSNs and MSNs-GA's cytotoxicity and free GA on larynx cancer cells is necessary. The different formulations were incubated at different concentrations of 0-10000 (µg/ ml) for (72 h) and evaluated using 3-[4,5-dimethylthiazol-2-yl]-2, 5-diphenyltetrazolium bromide (MTT) reduction. In (96) well plates, larynx cancer cells were seeded. Followed by 24 hours of incubator incubation at 37 degrees Celsius. Decanting growth medium (relative humidity (95%) and CO_2 (5%)). Sonicating DMEM with different amounts of MSNs, MSNs-GA, and free GA (0-10000 g/ ml) for 20 minutes. After that, (100µl) of the different prepared concentrations of MSNs, MSNs-GA, and GA were added into the cell and incubated for 72 hours. At the end of the incubation, 25 µl of MTT 0.5% was added to each well. The plates were then incubated for another three hours at 37°C. After removing the medium, 0.05 ml of Dimethyl sulphoxide (DMSO) was added to each well for 30 minutes. The plates were then placed in the shaker for 30 minutes to dissolve the crystals of dark blue formazan. Platform readers were used to measure the plates' absorbance at a wavelength of 570 nm. According to this formula, cell viability was measured as a percentage:

$$\text{cell viability} = ((Abs570 \text{ treated cells})/ (Abs570 \text{ control cells})) *100\%$$

2.3.6. Statistical analysis

The data generated in this study were derived from a minimum of three independent experiments, and the outcomes were expressed as the mean ± standard deviation (SD). Statistical analyses, including comparisons for both independent and dependent materials, were performed using SPSS version 26.

3. Results

3.1. Drug Encapsulation Efficiency

For MSN1, MSN2, and MSN3, the drug loading efficiencies were 99.9%, 99.84%, and 99.70%, respectively. These

findings demonstrated the successful encapsulation of the medication. and we observed the small size of msns

3.2. Characterization of MSNs

3.2.1. Particle size

Particle size distributions for the various formulations are depicted in Fig. 1. MSN1(178.3±2.51) nm, MSN2 (186±37.3) nm, MSN3 (241±32.5) nm, MSN1-GA (329.1±92.9) nm, MSN2-GA (337.7±42.10) nm and MSN3-GA (356.4 ±112.3) nm. NH4OH accelerated hydrolysis and polymerization rates and sped up the reaction kinetics, resulting in larger particle sizes [43]. The effects of the amounts of NH_3OH on the particle size of MSNs are shown in Fig. 2. The PDI (polydispersity index distribution) was MSN1 (0.44), MSN2 (0.37), MSN3(0.54), MSN1-GA (0.48), MSN2-GA (0.28), and MSN3-GA (0.51). PDI (polydispersity index) evaluates the uniformity and homogeneity of the nanoparticles' size. PDI value between 0.1 and 0.5 suggests a relatively narrow dispersion. When the PDI is more than 0.5, there is a wide dispersion. [45]. The narrowest PDI width focuses on colloidal stability and demonstrates suitability for use as a drug delivery system via systemic therapy [46]. The PDI value denotes monodispersed and uniform formulations [43].

3.2.2. Zeta potential

It was determined that the average zeta potential of several unloaded formulations was -31.4 mv, -35.6 mv, and -24.2 mv for MSN1, MSN2, and MSN3, respectively these results indicate the colloidal stability of MSN1, MSN2, and MSN3 resist aggregation and The surface hydroxyl groups of the MSNs were given a negative zeta potential. [50, 51]. At the same time, those for loaded formulations were found to be -19.9 mV, -15.5 mV, and -12.9 mV for MSN1-GA, MSN2-GA, and MSN3-GA, respectively, these results refer to the possible aggregation of nanoparticles and zeta potential values of all MSNs decrease with increasing nanoparticle size. as shown in Fig. 3.
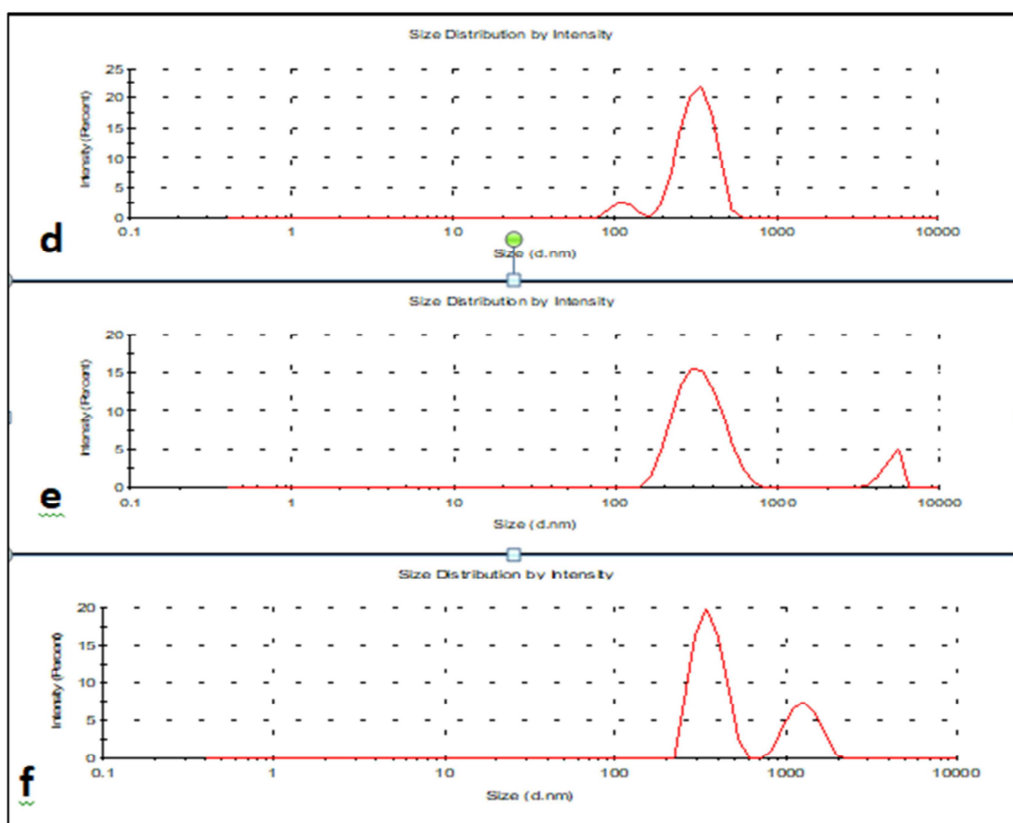
.

_____

_____

Figure 1: Particle size distribution of the different mesoporous silica nanoparticles and gallic acid-loaded mesoporous silica nanoparticles formulations, The PDI value denotes monodispersed and uniform formulations (a) MSN1, (b) MSN2, (c) MSN3, (d) MSN1-GA, (e) MSN2-GA, (f) MSN3-GA.
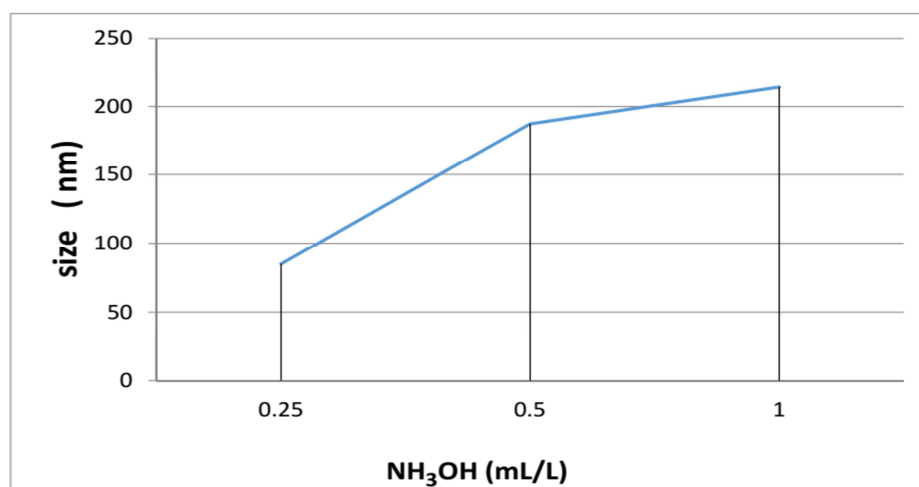

Figure 2: Effects of the amounts of NH3OH on the particle size of MSNs observed an increase in the size with the increase of NH_3OH
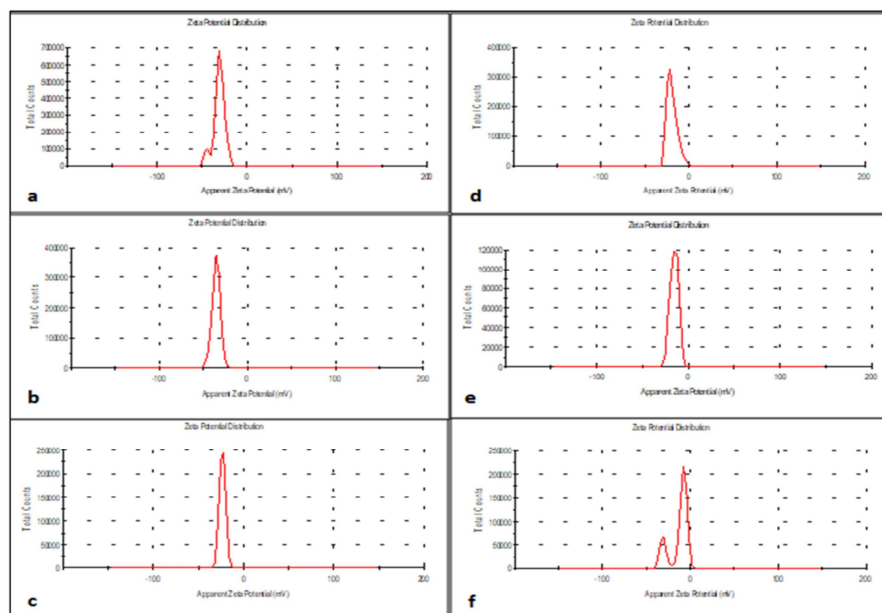
Figure 3: Zeta potential of the different mesoporous silica nanoparticles and gallic acid-loaded mesoporous silica nanoparticle formulations these results indicate the colloidal stability of(a) MSN1; (b) MSN2; (c) MSN3; (d) MSN1-GA;(e)MSN2-GA; (f) MSN3-GA.

3.2.3. SEM micrographs

Micrographs taken with a scanning electron microscope reveal the presence of uniformly sized spheres (Philips XL-30) SEM shows that MSNs are regular spherical particles that are generally homogeneous. The average size of these MSNs is 84 nm,187 nm, and 214 nm, respectively, as shown in Fig.4.
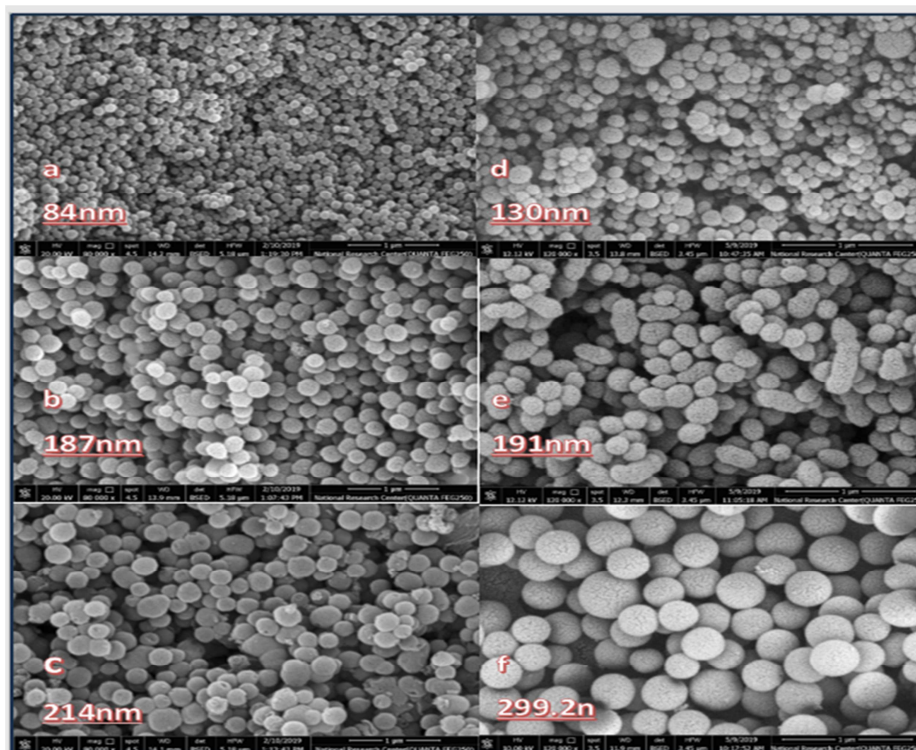

Figure 4: SEM images of Mesoporous silica nanoparticles show regular spherical particles that are generally homogeneous
(a) MSN1, (b) MSN2, (c) MSN3,(d) MSN1-GA, (e) MSN2-GA, (f) MSN3-GA

_____

3.2.4. In vitro release study of GA

     Nanoparticles were produced and loaded with GA to determine the optimal conditions for preparation in drug delivery applications. Figure 5 displays the cumulative drug release across all samples. The drug release rate for MSN1, which is 84 nm in size and has an EE of 99.9%, was 29% during the first four hours and gradually decreased after that. The initial four hours of drug release were the fastest (38%) and 40%) for MSN2 and MSN3 with size (178 nm and 214 nm) and high EE (99.89% and 99.70%), respectively. This result indicates that the firing rate of GA from MSN1 is lower than that of MSN2 and MSN3.
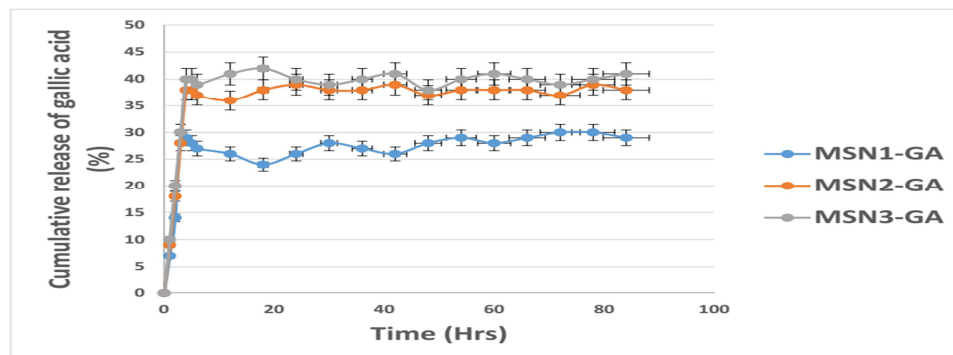

Figure 5: Cumulative release of GA from prepared MSN 1 showed low drug release while the release of MSN2 and MSN3 showed the highest drug release.

3.2.5 MTT assay

This test was essential to estimate the cytotoxicity of different sizes of MSNs, MSNs -GA containing (40 mg/ml) of GA compared to free GA. The cellular uptake efficiency was determined after incubation with HEP2 cells at different concentrations (10000-4.488 µg/ ml) for 72 hours of incubation. the MTT assay showed that GA no toxicity was observed at (4.8-19.5 µg/ ml) after that the cell viability of HEP-2 cells decreased in a dose- and time-dependent manner; and we observed no toxicity at the low concentration for MSN1 (4.488-312.5 µg/ ml) while the concentration increase, we observed low toxicity; after loaded GA we observed MSN1-GA show no toxicity at the low concentration (4.488-156.25 µg/ ml) and an increase of the concentration the toxicity increased. For MSN2 (4.488-312.5 µg/ ml) no toxicity at the low concentration was observed but the toxicity was increased at high concentration. while at the biggest size of MSN3, we observed no toxicity at (4.488-78.125 µg/ ml) and high toxicity at high concentrations. these results indicate that the cell viability of HEP2 decreased at high concentrations of MSNs as shown in Fig .6. (a) but for MSN2-GA and MSN3-GA the cell viability of HEP2 decreased at high concentrations begins to decrease at low concentrations as shown in Fig .6. (b). The IC50 value is the concentration of medication at which 50% of cells die after a given period. A lower IC50 value indicates more cytotoxicity [54]. GA as a positive control has the lowest IC50 value and exhibited the most potent cytotoxicity on HEP-2 cancer cells which is estimated to be (183 µg/ml), (634 µg/ml) MSN1-GA, (704 µg/ml) MSN2-GA, (773.9 µg/ml) MSN3-GA (774 µg/ml) MSN1, (1210 µg/ml) MSN2 and (371.38 µg/ml) MSN3 for 72 h incubation, respectively as shown in Fig .7. (a,b). The cell viability of GA was estimated to be 17.3, 72.3, and 100%; MSN1 was estimated to be 26.9, 100 and 100 %, MSN2 was estimated to be 32,100 and 100%; and MSN3 was estimated to be 49, 99 and 100 %, For MSN1-GA, the cell viability was estimated to be 41.50,100 and 100 %. , MSN2-GA, the cell viability was estimated to be 32, 93, and 100 %, and for MSN3-GA, 27.37, 82, and 100 %, the cell viability of HEP2 decreased at high concentration begins to decrease at low concentrations as shown in Fig .6. (b).
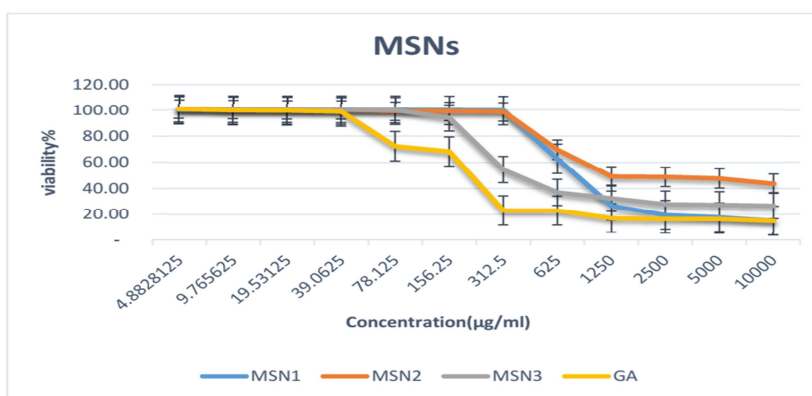

Figure 6: (a) The Viability of HEP2 after 72 h of incubation with MSN1, MSN2, and MSN3 at different concentrations (4.9, 9.8, 19.5, 39.1, 78.1, 156.3, 312.5, 625, 1250, 2500, 5000, 10000) µg/ml decreased with the increased of the concentration.
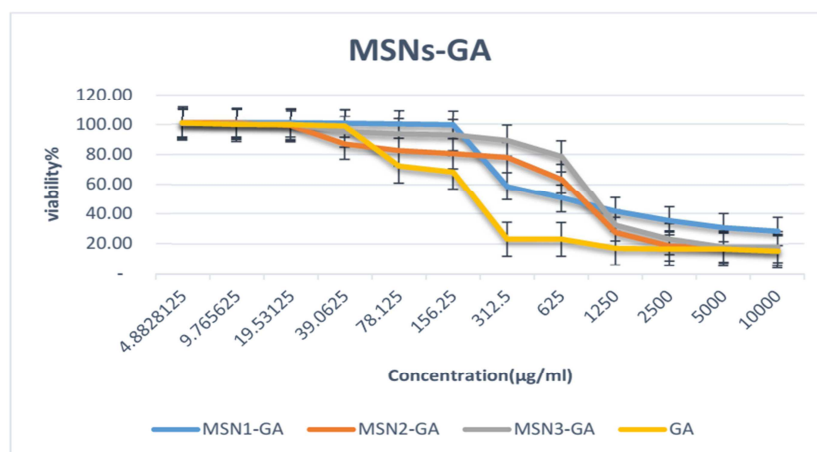
_____

Figure 6: (b) The Viability of HEP2 after 72 h of incubation withMSN1-GA, MSN2-GA, and MSN3-GA at different concentrations (4.9, 9.8, 19.5, 39.1, 78.1, 156.3, 312.5, 625, 1250, 2500, 5000, 10000) µg/ml decreased with the increased of the concentration.
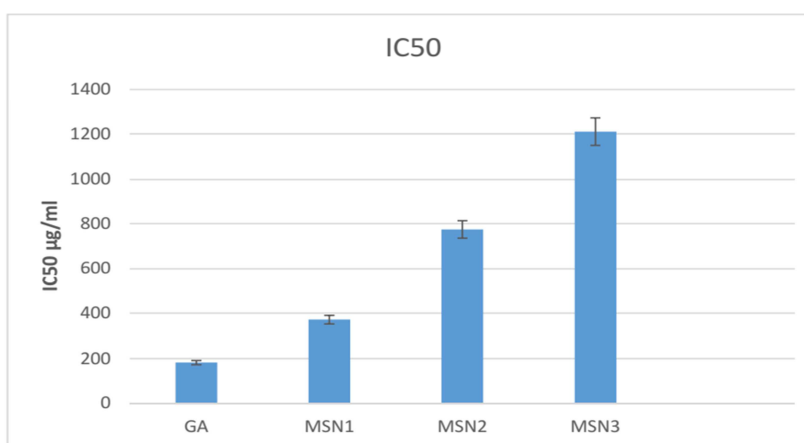

Figure 7: (a) IC_{50} values for MSN1 nanoparticles showed more significant cytotoxicity on HEP-2 cancer cells than MSN2 and MSN3
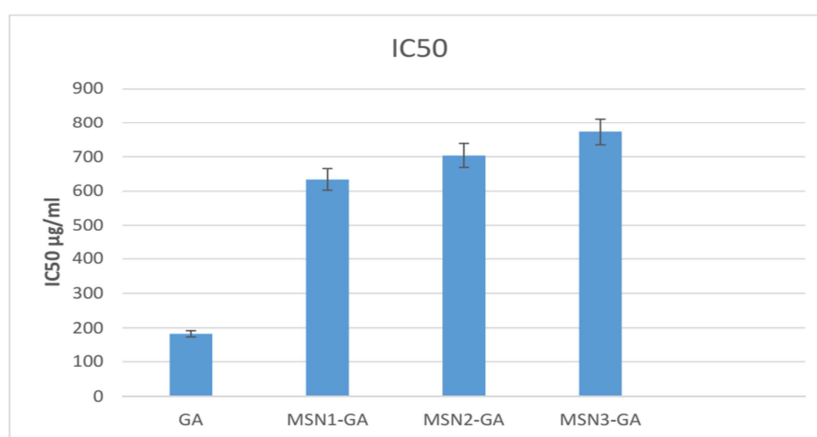

Figure 7: (b) IC_{50} values for MSN1-GA nanoparticles showed more significant cytotoxicity on HEP-2 cancer cells than MSN2-GA and MSN3-GA

3.2.6. Statistical analysis

In the present study, as detailed in Table 1, we observed varying levels of cytotoxicity in HEP-2 cells when exposed to different concentrations of MSN1, MSN2-GA, and MSN3-GA . At 10000, 5000, and 2500 µg/ml concentrations, MSN1, MSN2-GA, and MSN3-GA demonstrated a non-significant increase in cytotoxicity relative to the control group. In contrast, significant increases in cytotoxicity were observed for MSN2, MSN3, and MSN1-GA. Similarly, at a concentration of 1250 µg/ml, MSN1, MSN2-GA, and MSN3-GA showed a non-significant increase in cytotoxicity relative to the control group, while MSN2, MSN3, and MSN1-GA demonstrated significant increases. At lower concentrations of 625 and 312.5 µg/ml, MSN1, MSN2, and MSN3-GA did not show an increase in cytotoxicity relative to the control group. However, significant increases in cytotoxicity were observed for MSN3, MSN1-GA, and MSN2-GA. Finally, at a concentration of 156.2 µg/ml, MSN2, MSN3, MSN2-GA, and MSN3-GA showed non-significant increases in cytotoxicity relative to the control group. In contrast, significant increases were observed for MSN1 and MSN1-GA, and at a concentration of 78.12 µg/ml, MSN1-GA, MSN2-GA, and MSN3-GA exhibited non-significant increases in cytotoxicity, while significant increases were observed in HEP-2 cells compared to the control group for MSN1, MSN2, and MSN3. At a concentration of 39.06 µg/ml, MSN3, and MSN1-GA showed non-significant increases in cytotoxicity, while MSN2-GA and MSN3-G displayed non-significant decreases. However, significant increases in cytotoxicity were observed in HEP-2 cells compared to the control group for MSN1 and MSN2. At a concentration of 19.35 µg/ml, MSN1, MSN2, MSN3, and MSN1-GA showed non-significant increases in cytotoxicity, while MSN2-GA and MSN3-G showed non-significant decreases in HEP-2 cells compared to the control group.

At a concentration of 9.76 µg/ml, MSN3, MSN1-GA, and MSN2-GA showed non-significant increases in cytotoxicity, while MSN3-GA showed a non-significant decrease. However, significant increases in cytotoxicity were observed in HEP-2 cells compared to the control group for MSN1 and MSN2. Finally, at a concentration of 4.882 µg/ml, MSN3, MSN1-GA, MSN2-GA, and MSN3-GA showed non-significant increases in cytotoxicity in HEP-2 cells compared to the control group, while significant increases were observed for MSN1 and MSN2. These results are illustrated in Figure 8.a&b.

Table 1: Statistical Analysis: Impact of Cytotoxicity Induced by Free GA, MSN1, MSN2, MSN3, GA-MSN1, GA-MSN2, and GA-MSN3 on HEP-2 Cells across 12 Distinct Concentrations; * Denotes Significant Heterogeneity at P <0.05.

|	Control	MSN1		MSN2		MSN3		MSN1-GA		MSN2-GA		MSN3-GA	
	mean ±S.E.M	mean ±S.E.M	D%	mean ±S.E.M	D%	mean ±S.E.M	D%	mean ±S.E.M	D%	mean ±S.E.M	D%	Mean ±S.E.M	D%
10000	0.06 ± 0.001^a	0.06 ± 0.003^a	0	0.14 ± 0.03^b	133	0.16 ± 0.01^b	167	0.14 ± 0.003^b	133	0.07 ± 0.004^a	17	0.06 ± 0.002^a	0
5000	0.06 ± 0.003^a	0.07 ± 0.01^a	17	0.14 ± 0.006^b	133	0.18 ± 0.01^b	200	0.16 ± 0.024^b	167	0.07 ± 0.004^a	17	0.07 ± 0.003^a	17
2500	0.06 ± 0.003^a	0.07 ± 0.014^a	17	0.14 ± 0.03^b	133	0.18 ± 0.01^b	200	0.18 ± 0.003^b	200	0.09 ± 0.003^a	50	0.07 ± 0.01^a	17
1250	0.07 ± 0.01^d	0.1 ± 0.02^{ad}	43	0.17 ± 0.01^{ac}	143	0.18 ± 0.01^{bc}	157	0.21 ± 0.01^{ae}	200	0.12 ± 0.006^{de}	71	0.11 ± 0.01^d	57
625	0.09 ± 0.03^b	0.23 ± 0.02^{ab}	156	0.19 ± 0.05^{ab}	111	0.26 ± 0.04^a	189	0.26 ± 0.01^a	189	0.30 ± 0.03^a	233	0.24 ± 0.03^{ab}	167
312.5	0.09 ± 0.01^b	0.4 ± 0.06^{ab}	344	0.28 ± 0.08^{ab}	211	0.41 ± 0.02^a	356	0.3 ± 0.03^a	233	0.34 ± 0.01^a	278	0.30 ± 0.02^{ab}	233
156.2	0.26 ± 0.02^b	0.53 ± 0.04^{ac}	104	0.48 ± 0.06^{ab}	85	0.44 ± 0.05^{ab}	69	0.58 ± 0.04^a	123	0.35 ± 0.02^{ab}	35	0.31 ± 0.07^{bc}	19
78.12	0.27 ± 0.05^b	0.67 ± 0.05^a	148	0.67 ± 0.08^a	148	0.55 ± 0.04^{ac}	104	0.58 ± 0.08^{bc}	115	0.36 ± 0.02^{bc}	33	0.31 ± 0.05^b	15
39.06	0.37 ± 0.04^b	0.72 ± 0.08^a	95	0.7 ± 0.07^a	89	0.59 ± 0.03^{ab}	59	0.63 ± 0.04^{ab}	70	0.36 ± 0.04^b	-3	0.33 ± 0.1^b	-11
19.53	0.42 ± 0.08^{ab}	$0.73\pm.08^{ab}$	74	0.76 ± 0.09^a	81	0.60 ± 0.07^{ab}	43	0.62 ± 0.04^{ab}	48	0.41 ± 0.03^b	-2	0.38 ± 0.1^{ab}	-10
9.76	0.43 ± 0.02^b	0.76 ± 0.06^a	77	0.82 ± 0.06^a	91	0.63 ± 0.02^{ab}	47	0.65 ± 0.04^{ab}	51	0.44 ± 0.02^b	2	0.41 ± 0.1^b	-5
4.882	0.44 ± 0.02^b	0.79 ± 0.04^a	80	0.83 ± 0.03^a	89	0.64 ± 0.0^{ab}	45	0.66 ± 0.04^{ab}	50	0.51 ± 0.08^b	16	0.49 ± 0.005^b	11
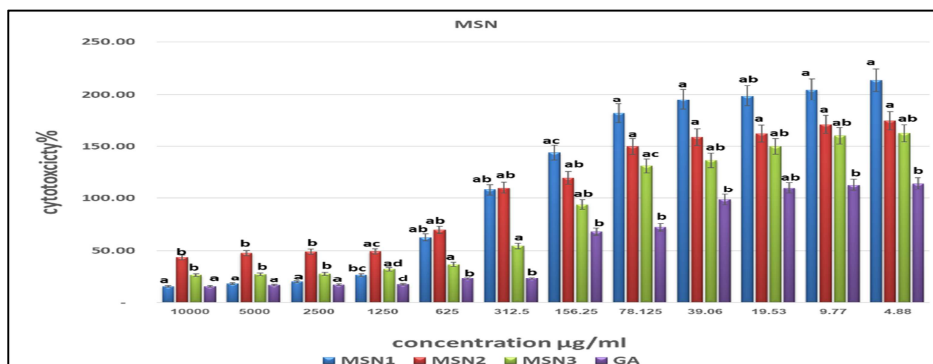
Figure 8: (a) Effect of cytotoxicity of free GA, MSN1, MSN2, MSN3 and GA-MSN3 on the (HEP-2) in 12 different concentrations; * significant heterogeneity at P <0.05
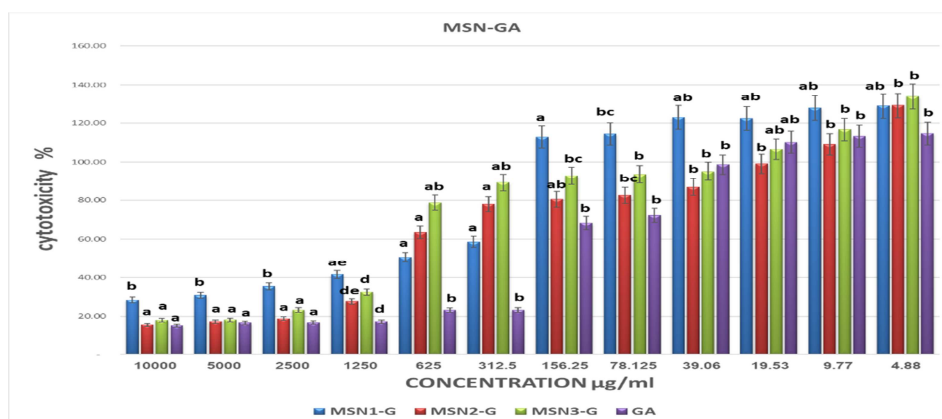
Figure 8: (b) Effect of cytotoxicity of free GAGA-MSN1, GA-MSN2and GA-MSN3 on the (HEP-2) in 12 different concentrations; * significant heterogeneity at P <0.05

4. Discussion

The Stöber method is a chemical process that is frequently used to produce monodisperse (uniform-sized) silica particles [39]. This procedure was developed by German scientist W. Stöber in the 1960s., involves the treatment of tetraethyl orthosilicate (TEOS) in an alcoholic solution by hydrolysis and condensation, often with the use of a base catalyst such as ammonium hydroxide, which facilitates the hydrolysis of (TEOS) into silicic acid. (NH₄OH) plays a crucial role in controlling the size and uniformity of the mesoporous silica nanoparticles (MSNs). [**40, 41,42**] NH4OH accelerated hydrolysis and polymerization rates and sped up the reaction kinetics, resulting in larger particle sizes the growth rate and final size of the nanoparticles are determined by the rates of hydrolysis and condensation. [**43**]. The inclusion of the hydration layer created surrounding the nanoparticles when introduced in a media may account for the larger size of MSNs acquired using the DLS approach as compared to that obtained using the SEM [**44**] [56]**.** The effect of ammonia concentration on the PDI of MSN first decreased and then increased when the ammonia concentration increased from 0.25 ml/L to 1 ml/L value [**43**]; when adding ammonia, the hydrolysis reaction represented a nucleophilic reaction, with the hydroxyl attacking the silica molecule of TEOS and producing silicic acid. Under alkaline conditions, silicic acid loses its hydrogen and attacks another silica molecule, resulting in a condensation reaction. Because there were fewer intermediates in this process, the hydrolytic rate was faster than the condensation rate, thus dominating the reaction rate. As the concentration of ammonia increased, the hydrolytic rate increased, which increased the MSN particle size [**47**]**.**Zeta Potential is a good measure of how much colloidal particles interact with each other, and it is used to figure out how stable colloidal systems are [**48**]. The strength of electrostatic repulsion between neighboring, similarly charged particles is proportional to the zeta potential of the dispersion. A solution or dispersion with a high zeta potential will contain stable molecules or particles that do not stick together. Due to the low potential, the attractive forces are more potent than the repulsive ones. Another possibility is that the dispersion is disrupted and flocculated. The physical stability of the preparations is confirmed by greater Zeta values, which imply a more substantial surface charge and prevent the aggregation of the nanoparticles [**49**]**.**the colloidal stability in this research the result of Zeta Potential indicates the colloidal stability of MSN1, MSN2, and MSN3 resist aggregation and The surface hydroxyl groups of the MSNs were given a negative zeta potential, while After GA loading in MSN, the charge of MSN1-GA, MSN2-GA, and MSN3-GA also became negative. Still, the magnitude decreased these results refer to the possible aggregation of nanoparticles and zeta potential values of all MSNs decrease with increasing nanoparticle size [**50, 51**]   Hydrogen bonding occurred between the carboxyl group of GA and the Si-OH groups of silica, enclosing GA within the pores of MSNs. The integration of the drug into the nanoparticle must be responsible for the growth in size following drug loading. All samples of MSN indicate a high drug encapsulation level in the nanoparticle. The MSN1 cumulative drug release profile was the lowest at the predetermined time points. Despite its high loading, the MSN1 sample showed deficient drug release. The low rate of drug release seemed to be due to the association of the drug and the tiny silica pores of MSN1 .These features would be favorable, except for the release. MSN2 and MSN3   showed the highest drug release, which implied that they would not be preferred for drug delivery applications because drugs cannot be stored in their pores for a long time. Therefore, the drug might be released into the biological system before reaching the target cell [**52**]. MSNs were used to carry chemical substances as nanocarriers to increase their bioavailability. Because of the poor absorption, low bioavailability, and rapid metabolism of Gallic acid (GA), it has low bioavailability which contribute to its fast removal [20]; therefore, it has been suggested to encapsulate GA in nanoparticles to efficiently enhance their bioavailability and improve their therapeutical results in cancer tissues through increasing absorption by transcellular or paracellular mechanisms [**38,20**] Evaluating the toxicity of nanoparticles to cancer cells is a beneficial technique The potential toxicity of nanoparticles could significantly vary depending on changes in their physical-chemical characteristics, such as diameter size, a charge on the surface, and morphology. Smaller nanoparticles may be more reactive in biological systems because they have more significant surface areas; higher surface activities in smaller sizes could facilitate cellular uptake, tissue penetration, and systemic distribution Therefore, Smaller MSNs are characterized by a larger surface area and higher surface reactivity, which may render them more active chemically and biologically [**53**]**.** Consequently, the toxicity caused increases as the particle size decreases. This was the outcome of the MTT test in this

_____

research, which showed that the dose and duration of exposure to GA reduced the cell viability of HEP-2 cancer. Cell viability decreased with time and increasing concentrations of free GA [55], MSN1 possesses a greater surface area to volume ratio, allowing them to interact with biological tissues and cells on a greater level. Their greater surface area may raise their reactivity and potential for harm, and it may make it easier for them to pass through cellular membranes, thus increasing their toxicity and having more profound intracellular effects so it was more suitable for enhancing the effect of GA to treat laryngeal cancer   compared to the MSN2 and MSN3. [56].

5. Conclusion

Mesoporous silica nanoparticles (MSNs) of varying sizes were synthesized by the Stöber method and characterized the conclusion of our observations that larger particles are generated faster due to faster hydrolysis and condensation, an increase in ammonia concentration also causes the MSNs to grow in size. These MSNs were used as nanocarriers to carry the powerful anticancer drug gallic acid (GA). High encapsulation efficiency for GA was demonstrated by smaller MSN1mor than MSN2 and MSN3. HEP-2 cells exhibited cytotoxicity uptake of GA-loaded MSNs across a range of concentrations (4.88-10000 µg/ml). On HEP-2 cells, the smaller MSN1 showed good encapsulation efficiency for GA and lower toxicity than MSN2 and MSN3. However, after being loaded with GA, MSN1 showed noticeably higher toxicity than MSN2 and MSN3 loaded with GA. In conclusion, due to their small size and high encapsulation efficiency, MSNs emerge as ideal nanocarriers for GA delivery, presenting a promising therapeutic strategy for treating laryngeal carcinoma cells.

Declaration

Ethics approval and consent to participate

Not applicable

Consent for publication

Not applicable

Data availability

All data needed to support the conclusions are included in this article. Additional data related to this paper can be requested from the author (hfahmy@sci.cu.edu.eg)

Authors' contributions

H.M.F.& A.S.M designed this study, and M.M.H wrote the main manuscript, performed the experiments, and prepared Figs. All authors reviewed the manuscript. All authors read and approved the final manuscript.

Conflict of interest

The authors declare that they have no competing interests.

Funding

Not applicable

6. References

(1) Igissin, N., Zatonskikh, V., Telmanova, Z., Tulebaev, R., & Moore, M. (2023). Laryngeal cancer: Epidemiology, etiology, and prevention: A narrative review. *Iranian journal of public health*, *52*(11), 2248. https://doi: 10.18502/ijph.v52i11.14025

(2) Dancey, J. E., Bedard, P. L., Onetto, N., & Hudson, T. J. (2012). The genetic basis for cancer treatment decisions. *Cell*, *148*(3), 409-420.:https://doi.org/10.1016/j.cell.2012.01.014

(3) Bakrim, S., El Omari, N., El Hachlafi, N., Bakri, Y., Lee, L. H., & Bouyahya, A. (2022). Dietary Phenolic Compounds as Anticancer Natural Drugs: Recent Update on Molecular Mechanisms and Clinical Trials. *Foods*, *11*(21), 3323. https://doi.org/10.3390/foods11213323/

(4) Bhuia, M. S., Rahaman, M. M., Islam, T., Bappi, M. H., Sikder, M. I., Hossain, K. N., ... & Sharifi-Rad, J. (2023). Neurobiological effects of gallic acid: current perspectives. *Chinese Medicine*, *18*(1), 27 https:// doi.org /10.1186/s13020-023-00735-7

(5) Dhianawaty, D., Nurfazriah, L. R., & Rezano, A. (2020). Gallic Acid Content and Antioxidant Activity of Pomegranate Peel Ethanol Extract. *Majalah Kedokteran Bandung*, *52*(4), 243-248 https:// doi.org /10.15395/mkb.v52n4.2108

(6) Khodaie, F., & Ghoreishi, S. M. (2021). Experimental extraction of gallic acid from brown sumac seed (Rhus coriaria) using supercritical carbon dioxide and ethanol as co-solvent: Modeling and optimization. *The Journal of Supercritical Fluids*, *175*, 105266. https:// doi.org /10.1016/j.supflu.2021.105266

(7) Velho, P., Rebelo, C. S., & Macedo, E. A. (2023). Extraction of Gallic Acid and Ferulic Acid for Application in Hair Supplements. *Molecules*, *28*(5), 2369. 950. https:// doi.org /10.3390/molecules28052369

(8) Liu, Y. L. *et al.* Gallic acid attenuated LPS-induced neuroinflammation: protein aggregation and necroptosis. *Mol. Neurobiol.* 57, 96–104 (2020). https:// doi.org /10.1007/s12035-019-01759-7

(9)Aborehab, N. M., & Osama, N. (2019). Effect of Gallic acid in potentiating chemotherapeutic effect of Paclitaxel in HeLa cervical cancer cells. *Cancer cell international*, *19*, 1-13. https://doi.org/10.1186/s12935-019-0868-0

(10)Gülçin, İ., Huyut, Z., Elmastaş, M., & Aboul-Enein, H. Y. (2010). Radical scavenging and antioxidant activity of tannic acid. *Arabian journal of chemistry*, *3*(1), 43-53. https://doi.org/10.1016/j.arabjc.2009.12.008

(11) Drews, J. (2000). Drug discovery: a historical perspective. *science*, *287*(5460), 1960-1964. https://doi:10.1126/science.287.5460.1960

(12) Jafarinejad, S., Martin, W. H., Ras, B. A., Isreb, M., Jacob, B., Aziz, A., ... & Najafzadeh, M. (2024). The anticancer/cytotoxic effect of a novel gallic acid derivative in non-small cell lung carcinoma A549 cells and peripheral blood mononuclear cells from healthy individuals and lung cancer patients. *BioFactors*, *50*(1), 201-213. https://doi.org/10.1002/biof.2003

_____

_____

(13) Alves, A. D. C. S., Mainardes, R. M., & Khalil, N. M. (2016). Nanoencapsulation of gallic acid and evaluation of its cytotoxicity and antioxidant activity. *Materials Science and Engineering: C*, *60*, 126-134. https://doi.org/10.1016/j.msec.2015.11.014

(14) Yang, K., Zhang, L., Liao, P., Xiao, Z., Zhang, F., Sindaye, D., ... & Deng, B. (2020). Impact of gallic acid on gut health: focus on the gut microbiome, immune response, and mechanisms of action. Front Immunol 11: 580208 https:// doi.org /10.3389/fimmu.2020.580208

(15) Wianowska, D., & Olszowy-Tomczyk, M. (2023). A Concise Profile of Gallic Acid—From Its Natural Sources through Biological Properties and Chemical Methods of Determination. *Molecules*, *28*(3), 1186. https:// doi.org /10.3390/molecules28031186.

(16) Bhuia, M. S., Rahaman, M. M., Islam, T., Bappi, M. H., Sikder, M. I., Hossain, K. N., ... & Sharifi-Rad, J. (2023). Neurobiological effects of gallic acid: Current perspectives. *Chinese Medicine*, *18*(1), 27.https://doi.org/10.1186/s13020-023-00735-7

(17) Inoue M, Sakaguchi N, Isuzugawa K, Tani H, Ogihara Y (2000) Role of reactive oxygen species in gallic acid-induced apoptosis. Biol Pharm Bull 23:1153–1157 https:// doi.org /10.1248/bpb.23.1153

(18) Shi, C. J., Zheng, Y. B., Pan, F. F., Zhang, F. W., Zhuang, P., & Fu, W. M. (2021). Gallic acid suppressed tumorigenesis by an LncRNA MALAT1-Wnt/β-catenin axis in hepatocellular carcinoma. *Frontiers in Pharmacology*, 2517. https:// doi.org /10.3389/fmolb.2020.00193

(19) Huang, P. J., Hseu, Y. C., Lee, M. S., Kumar, K. S., Wu, C. R., Hsu, L. S., ... & Yang, H. L. (2012). In vitro and in vivo activity of gallic acid and Toona sinensis leaf extracts against HL-60 human premyelocytic leukemia. *Food and chemical toxicology*, *50*(10), 3489-3497. https:// doi.org /10.1016/j.fct.2012.06.046

(20) Alves, A. D. C. S., Mainardes, R. M., & Khalil, N. M. (2016). Nanoencapsulation of gallic acid and evaluation of its cytotoxicity and antioxidant activity. *Materials Science and Engineering: C*, *60*, 126-134. https:// doi.org /10.3389/fphar.2021.708967

(21) Yao, Y., Zhou, Y., Liu, L., Xu, Y., Chen, Q., Wang, Y., ... & Shao, A. (2020). Nanoparticle-based drug delivery in cancer therapy and its role in overcoming drug resistance. *Frontiers in molecular biosciences*, 7, 193. https:// doi.org /10.3389/fmolb.2020.00193

(22) Watermann, A., & Brieger, J. (2017). Mesoporous silica nanoparticles as drug delivery vehicles in cancer. *Nanomaterials*, *7*(7), 189. https:// doi.org /10.3390/nano7070189

(23) Trzeciak, K., Chotera-Ouda, A., Bak-Sypien, I. I., & Potrzebowski, M. J. (2021). Mesoporous silica particles as drug delivery systems—The state of the art in loading methods and the recent progress in analytical techniques for monitoring these processes. *Pharmaceutics*, *13*(7), https:// doi.org /10.3390/pharmaceutics13070950

(24) Fang, L., Zhou, H., Cheng, L., Wang, Y., Liu, F., & Wang, S. (2023). The application of mesoporous silica nanoparticles as a drug delivery vehicle in oral disease treatment. *Frontiers in Cellular and Infection Microbiology*, *13*, 81. https://doi.org/10.3389/fcimb.2023.1124411

(25) Slowing, I. I., Vivero-Escoto, J. L., Wu, C. W., & Lin, V. S. Y. (2008). Mesoporous silica nanoparticles as controlled release drug delivery and gene transfection carriers. *Advanced drug delivery reviews*, *60*(11), 1278-1288 https:// doi.org /10.1016/j.addr.2008.03.012

(26) Rastegari, E., Hsiao, Y. J., Lai, W. Y., Lai, Y. H., Yang, T. C., Chen, S. J., ... & Chien, Y. (2021). An Update on Mesoporous Silica Nanoparticle Applications in Nanomedicines. Pharmaceutics 2021, 13, 1067. https:// doi.org /0.3390/pharmaceutics13071067

(27) Seljak, K. B., Kocbek, P., & Gašperlin, M. (2020). Mesoporous silica nanoparticles as delivery carriers: An overview of drug loading techniques. *Journal of Drug Delivery Science and Technology*, *59*, 101906. https:// doi.org /10.1016/j.jddst.2020.101906

(28) Maleki, A., Kettiger, H., Schoubben, A., Rosenholm, J. M., Ambrogi, V., & Hamidi, M. (2017). Mesoporous silica materials: From physico-chemical properties to enhanced dissolution of poorly water-soluble drugs. *Journal of Controlled Release*, *262*, 329-347. https:// doi.org / 10.1016/j.jconrel.2017.07.047

(29) Kolimi, P., Narala, S., Youssef, A. A. A., Nyavanandi, D., & Dudhipala, N. (2023). A systemic review on developing mesoporous nanoparticles as a vehicle for transdermal drug delivery. *Nanotheranostics*, *7*(1), 70-89. https:// doi.org /

(30) Kumar, P., Tambe, P., Paknikar, K. M., & Gajbhiye, V. (2018). Mesoporous silica nanoparticles as cutting-edge theranostics: Advancement from merely a carrier to the tailor-made smart delivery platform. *Journal of Controlled Release*, *287*, 35-57. https:// doi.org / 10.1016/j.jconrel.2018.08.024

(31) Wagner, J., Gößl, D., Ustyanovska, N., Xiong, M., Hauser, D., Zhuzhgova, O., ... & Bourquin, C. (2021). Mesoporous silica nanoparticles as pH-responsive carrier for the immune-activating drug resiquimod enhance the local immune response in mice. *ACS nano*, *15*(3), 4450-4466. https:// doi.org /10.1021/acsnano.0c08384

(32) Cheng, C. A., Chen, W., Zhang, L., Wu, H. H., & Zink, J. I. (2020). Magnetic resonance imaging of high-intensity focused ultrasound-stimulated drug release from a self-reporting core@ shell nanoparticle platform. *Chemical Communications*, *56*(71), 10297-10300. https:// doi.org /10.1039/D0CC03179H

(33) Joseph, M. M., Ramya, A. N., Vijayan, V. M., Nair, J. B., Bastian, B. T., Pillai, R. K., ... & Maiti, K. K. (2020). Targeted Theranostic Nano Vehicle Endorsed with Self-Destruction and Immunostimulatory Features to Circumvent Drug Resistance and Wipe-Out Tumor Reinitiating Cancer Stem Cells. *Small*, *16*(38), 2003309. https:// doi.org /10.1002/smll.202003309

(34) Lee, J. Y., Kim, M. K., Nguyen, T. L., & Kim, J. (2020). Hollow mesoporous silica nanoparticles with extra-large mesopores for enhanced cancer vaccine. *ACS applied materials & Interfaces*, *12*(31), 34658-34666. https:// doi.org /10.1021/acsami.0c09484

_____

(35) Tsamesidis, I., Pouroutzidou, G. K., Lymperaki, E., Kazeli, K., Lioutas, C. B., Christodoulou, E., ... & Kontonasaki, E. (2020). Effect of ion doping in silica-based nanoparticles on the hemolytic and oxidative activity in contact with human erythrocytes. *Chemico-Biological Interactions*, *318*, 108974. https:// doi.org /10.1016/j.cbi.2020.108974

(36) Ashour, M. M., Mabrouk, M., Soliman, I. E., Beherei, H. H., & Tohamy, K. M. (2021). Mesoporous silica nanoparticles prepared by different methods for biomedical applications: Comparative study. *IET nanobiotechnology*, *15*(3), 291-300. https:// doi.org /10.1049/nbt2.12023

(37) Kütük, N. (2021). Mesoporous silica nanoparticles, methods of preparation and use of bone tissue engineering. *International Journal of Life Sciences and Biotechnology*, *4*(3), 507-522.   https:// doi.org /10.38001/ijlsb.880711

(38) Anarjan, N., Tan, C. P., Nehdi, I. A., & Ling, T. C. (2012). Colloidal astaxanthin: Preparation, characterisation and bioavailability evaluation. *Food chemistry*, *135*(3), 1303-1309. https:// doi.org /10.1016/j.foodchem.2012.05.091

(39) Petrisor, G., Ficai, D., Motelica, L., Trusca, R. D., Bîrcă, A. C., Vasile, B. S., ... & Bleotu, C. (2022). Mesoporous silica materials loaded with gallic acid with antimicrobial potential. *Nanomaterials*, *12*(10), 1648. https:// doi.org /10.3390/nano12101648

(40) Lin, Y. S., & Haynes, C. L. (2010). Impacts of mesoporous silica nanoparticle size, pore ordering, and pore integrity on hemolytic activity. *Journal of the American Chemical Society*, *132*(13), 4834-4842. https:// doi.org /10.1021/ja910846q

(41) Zeng, D., Zhang, H., Wang, B., Sang, K., & Yang, J. (2015). Effect of ammonia concentration on silica spheres morphology and solution hydroxyl concentration in Stober process. *Journal of Nanoscience and Nanotechnology*, *15*(9), 7407-7411. https:// doi.org /10.1166/jnn.2015.10595

(42) Freidus, L. G., Kumar, P., Marimuthu, T., Pradeep, P., & Choonara, Y. E. (2021). Theranostic Mesoporous Silica Nanoparticles Loaded With a Curcumin-Naphthoquinone Conjugate for Potential Cancer Intervention. *Frontiers in Molecular Biosciences*, *8*, 670792. https:// doi.org /10.3389/fmolb.2021.670792

(43) Su, M., Su, H., Du, B., Li, X., Ren, G., & Wang, S. (2015). Mesoporous silica with monodispersed pores synthesized from the controlled self-assembly of silica nanoparticles. *Korean Journal of Chemical Engineering*, *32*(5), 852-859. https:// doi.org /10.1007/s11814-014-0270-5

(44) Zhang, Z., Mayoral, A., & Melián-Cabrera, I. (2016). Protocol optimization for the mild detemplation of mesoporous silica nanoparticles resulting in enhanced texture and colloidal stability. *Microporous and Mesoporous Materials*, *220*, 110-119. https:// doi.org /10.1016/j.micromeso.2015.08.026

(45) Wu, L., Zhang, J., & Watanabe, W. (2011). Physical and chemical stability of drug nanoparticles. Advanced drug delivery reviews, 63(6), 456-469. https://doi.org/10.1016/j.addr.2011.02.001

(46) Gisbert-Garzaran, M., Lozano, D., Matsumoto, K., Komatsu, A., Manzano, M., Tamanoi, F., & Vallet-Regí, M. (2021). Designing mesoporous silica nanoparticles to overcome biological barriers by incorporating targeting and endosomal escape. *ACS applied materials & interfaces*, *13*(8), 9656-9666. https:// doi.org /10.1021/acsami.0c21507

(47) Yan, Y., Fu, J., Xu, L., Wang, T., & Lu, X. (2016). Controllable synthesis of SiO2 nanoparticles: effects of ammonia and tetraethyl orthosilicate concentration. *Micro & Nano Letters*, *11*(12), 885-889. https:// doi.org /10.1049/mnl.2016.0434

(48) Ramaye, Y., Dabrio, M., Roebben, G., & Kestens, V. (2021). Development and Validation of Optical Methods for Zeta Potential Determination of Silica and Polystyrene Particles in Aqueous Suspensions. *Materials*, *14*(2), 290. https:// doi.org /10.3390/ma14020290

(49) Radwan, S. A. A., El-Maadawy, W. H., Yousry, C., ElMeshad, A. N., & Shoukri, R. A. (2020). Zein/phospholipid composite nanoparticles for the successful delivery of gallic acid into ahscs: influence of size, surface charge, and vitamin a coupling. *International journal of nanomedicine*, 7995-8018. https:// doi.org /10.2147/IJN.S270242

(50) Iraji, S., Ganji, F., & Rashidi, L. (2018). Surface-modified mesoporous silica nanoparticles as sustained-release gallic acid nanocarriers. *Journal of Drug Delivery Science and Technology*, *47*, 468-476. https:// doi.org /10.1016/j.jddst.2018.08.008

(51) Freidus, L. G., Kumar, P., Marimuthu, T., Pradeep, P., & Choonara, Y. E. (2021). Theranostic mesoporous silica nanoparticles loaded with a curcumin-naphthoquinone conjugate for potential cancer intervention. *Frontiers in molecular biosciences*, *8*, 670792. https:// doi.org /10.3389/fmolb.2021.670792

(52) Fathy, M. M., Yassin, F. M., Elshemey, W. M., & Fahmy, H. M. (2023). Insight on the Dependence of the Drug Delivery Applications of Mesoporous Silica Nanoparticles on Their Physical Properties. *Silicon*, *15*(1), 61-70. https:// doi.org / 10.2147/IJN.S436253

(53) Dong, X., Wu, Z., Li, X., Xiao, L., Yang, M., Li, Y., ... & Sun, Z. (2020). The size-dependent cytotoxicity of amorphous silica nanoparticles: a systematic review of in vitro studies. *International Journal of Nanomedicine*, 9089-9113. https:// doi.org /10.2147/IJN.S276105

(54) Berrouet, C., Dorilas, N., Rejniak, K. A., & Tuncer, N. (2020). Comparison of drug inhibitory effects (IC 50) in monolayer and spheroid cultures. *Bulletin of mathematical biology*, *82*(6), 68. https:// doi.org/10.1007/s11538-020-00746-7

(55) Rashidi, L., Vasheghani-Farahani, E., Soleimani, M., Atashi, A., Rostami, K., Gangi, F., ... & Tahouri, M. T. (2014). A cellular uptake and cytotoxicity properties study of gallic acid-loaded mesoporous silica nanoparticles on Caco-2 cells. *Journal of nanoparticle research*, *16*, 1-14. https:// doi 10.1007/s11051-014-2285

(56) Lehman, S. E., & Larsen, S. C. (2014). Zeolite and mesoporous silica nanomaterials: greener syntheses, environmental applications and biological toxicity. *Environmental Science: Nano*, *1*(3), 200-213. https:// doi.org 10.1039/C4EN00031E